

True-azimuth 3D Internal Multiple Attenuation without identifying the multiple generators

Barry Hung
 CGG
 Singapore
 barry.hung@cgg.com

Min Wang
 CGG
 Singapore
 min.wang@cgg.com

Malcolm Griffiths
 CGG
 Houston
 malcolm.griffiths@cgg.com

SUMMARY

We extend our previous work on 2D internal multiple attenuation without subsurface information to a 3D operation. We describe our implementation that involves selecting traces that honour the azimuth of acquisition for constructing multiple contribution gathers and then segmenting the chosen traces in a layer stripping fashion to predict internal multiple model without identifying the multiple-generating interfaces. We demonstrate through synthetic and field data examples that, by including crossline apertures in the prediction process and selecting traces with correct azimuths in the convolution and correlation processes, substantial improvement in image quality can be obtained for those data that exhibit the internal multiple problem.

Key words: 3D, true-azimuth, internal multiple.

INTRODUCTION

Internal multiple attenuation (IMA) has long been regarded as a challenging problem in seismic data processing. In contrast to surface related multiples which have received closer attention from researchers, primarily because of their relatively stronger effects on seismic migrated images and the ease of identifying their generators, internal multiples (IMs) tend to be regarded as a secondary issue even though it has been shown that complicated IMs do interfere with the interpretation of reservoirs (Griffiths et al., 2011). Recent developments in SRME such as 3D and true-azimuth (Lin et al., 2005; Moore and Bisley, 2005) applications have advanced the technology further. Since applying the concept of SRME to predict IMs is not a new idea, efforts have been spent in extending IMA to 3D application. Methods based on kinematic calculation using post-stack data (Reshef et al., 2006), model-driven wavefield extrapolation (Pica and Delmas, 2008), Jakubowicz's (1998) approach (Griffiths et al., 2011), ...etc., have been proposed. Nevertheless, most of these methods require a priori information about the subsurface.

Progress, however, has been made in addressing the need of identifying the multiple-generating interfaces for IMA. Approaches such as inverse scattering series (Weglein et al., 1997), layer-based method (Verschuur and Berkhout, 2005), window-based method (Hung and Wang, 2012; Retailleau et al., 2012) have been suggested for predicting IMs without subsurface information. However, besides the work of Retailleau et al., most of these approaches are limited to 2D

applications only. Therefore, the azimuth aspect of the data has not been explicitly considered. El-Emam et al. (2011) mentioned true-azimuth implementation for IMA but their approach applies to suppressing targeted IMs only.

In this paper, we extend our previous work from 2D to 3D operations to take into account the 3D nature of the earth's subsurface for predicting IMs without identifying the multiple-generating interfaces. In addition, we show how our method predicts IMs with true-azimuth geometries. We demonstrate that substantial improvement in image quality is obtained by including crossline aperture in the prediction process and selecting traces with correct azimuth in the convolution and correlation processes.

METHOD AND RESULTS

Following the work of Jakubowicz (1998), Griffiths et al. (2011) extended their 3D SRME workflow to handling IMs by identifying the multiple-generating horizons for muting the input data. As illustrated in Figure 1a, IM model that is specific to the horizon j can be predicted by Jakubowicz's convolution-correlation process using this equation:

$$\begin{aligned}
 M_j(x_r, y_r | x_s, y_s; f) &= \sum_{y_2^{aperture}} \sum_{x_2^{aperture}} \sum_{y_1^{aperture}} \sum_{x_1^{aperture}} D_m(x_r, y_r | x_1, y_1; f) \\
 &\otimes D_{m'}^*(x_1, y_1 | x_2, y_2; f) \otimes D_m(x_s, y_s | x_2, y_2; f) \quad (1)
 \end{aligned}$$

Where D_m and $D_{m'}$ are the data muted above and below a horizon (e.g. horizon k) just underneath horizon j , respectively; $D_{m'}^*$ is the complex conjugate of $D_{m'}$ and \otimes represents convolution operation. Two surface apertures, indicated by the dotted rectangles, are needed in this case to locate the two reflection points, I_1 and I_2 , to predict the multiple model M_j .

Recently, we have proposed a methodology, for 2D cases, to predict IMs without subsurface information by segmenting the data into different time windows for iteratively locating the top multiple-generating horizon (Hung and Wang, 2012). The same principle can be applied to model 3D IMs without identifying specific multiple-generating horizons. To fulfill the lower- higher-lower relationship (Weglein et al., 1997) that is crucial in the modeling of IMs, input data within the apertures is segmented into different windows, as shown in Figure 1b, in such a way that the window responsible for the downward reflections of the IMs (w_j) is always at a "higher" level (shorter traveltime) than the two windows that account for the upward reflections. With this implementation, all the IMs that have their top generators located within w_j can then be modeled. Repeating this operation to include possible deeper

top generators (i.e. using deeper window-segmented data consecutively), all IMs can be modeled without the need of identifying any 3D multiple-generating interface. This iterative process is equivalent to modifying Equation (1) as follows:

$$M(x_r, y_r | x_s, y_s; f) = \sum_{w_j=1}^{w_n} \sum_{y2_{aper}} \sum_{x2_{aper}} \sum_{y1_{aper}} \sum_{x1_{aper}} D_{w_k}(x_r, y_r | x_1, y_1; f) \otimes D_{w_j}^*(x_1, y_1 | x_2, y_2; f) \otimes D_{w_l}(x_s, y_s | x_2, y_2; f) \quad (2)$$

such that $w_k, w_l > w_j$

where D_{w_k} represents the segmented data that is muted off outside the time window w_k and the condition: $w_k, w_l > w_j$ indicates that D_{w_k} and D_{w_l} are the portions of data that have longer traveltimes than D_{w_j} . An extra summation term in Equation (2) is to ensure that all the possible multiple-generating horizons are taken into account in the process of predicting the IMs.

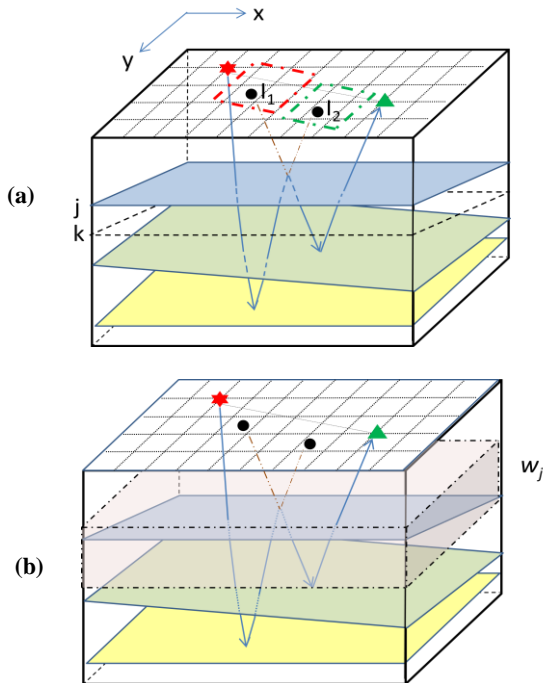


Figure 1. (a) Schematic diagram illustrating the generation of IM with the definition of two surface apertures indicated by the dotted rectangles. (b) Prediction of all IMs without identifying any multiple-generating horizons by window based top-down stripping of the top generators.

True-azimuth implementation

Just as important as in true-azimuth 3D SRME that appropriate traces need to be selected for constructing the multiple contribution gathers (MCGs), true-azimuth 3D internal multiple modeling involves careful selection and interpolation of traces to honor the aspects of azimuth, offset and midpoint in realizing Equation (2). The increase in the complexity in this case stems from the fact that two surface apertures are included within which the required traces are reconstructed for contributing to the MCG. To illustrate this, Figure 2 displays a plan view of 3D internal multiple prediction process. The shot and receiver positions of three pairs of required traces are indicated and the dotted lines represent the required azimuths and offsets. However, these

traces are seldom present in the regularized data. Depending on the selection criteria that may minimize the difference in azimuth, offset and midpoint, or weighted sum of these three, the nearest available traces are extracted from the input 3D shot and receiver gathers. Differential NMO is then used for correcting the discrepancy in offset and the resulting trace is rotated about the desired midpoint. In doing so, a tradeoff can be made in determining the relative importance of the three terms.

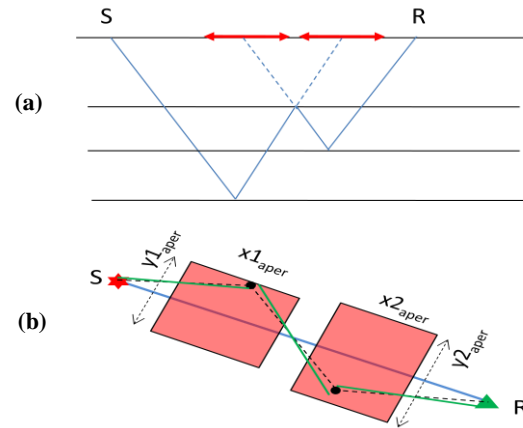


Figure 2. (a) Lateral view of the definition of the surface apertures. (b) Top view showing the azimuth of the desired traces (dotted lines) and the nearest available traces (green lines).

After three traces have been selected, they are then segmented according to their respective requirements in ensuring that the low-high-low relationship is fulfilled. In practice, for non-zero offset traces the windowing time is calculated based on normal moveout equation. Thus, hyperbolic events are assumed. Nevertheless, with not so complicated subsurface and the use of overlapping windows, it is valid to assume that all top generators are included in the process.

Examples

A 3D synthetic dataset was generated by acoustic wave-equation modeling using the velocity function (the density function has the same profile) shown in Figure 3a. Five events are present of which the top two events have significant dip in the crossline direction. The velocity and density profiles were modified so that identifiable IMs were generated. In this case, all the primary events are the generators of the multiples. Figure 3b depicts a portion of common offset volume where the primaries are indicated and the rest of the events are IMs (surface related multiples have been excluded in the modeling process). Without identifying the multiple-generating interfaces, the IM model predicted by our method using a y-aperture of 500m is depicted in Figure 4c. As a reference, the 2D model is shown in Figure 4b. The wiggle displays are the magnified overlaid sections that highlight the extent of matching between the input (coloured wiggle) and the models (black-and-white wiggle). It can be seen that, due to the out-of-plane contributions, the 3D model exhibits superior matching in the traveltimes with the input than the 2D model. Consequently, after performing adaptive subtraction, there is much more residual of the IMs left in the 2D result as depicted in Figure 4d than the 3D result in Figure 4c. To illustrate the importance of selecting traces with correct azimuth in forming the MCGs, Figure 5a shows a magnified section of a 3D IM model that was predicted by not honouring the azimuth aspect

of the target traces. Again, the input (coloured wiggle) is overlaid with the multiple model (black-and-white wiggle) and their mismatch in traveltimes is highlighted. In contrast, by minimising the difference in azimuth between the contributing traces and the target trace, Figure 5b displays a 3D IM model that aligns very well with the input.

The field data example comes from the Santos Basin, offshore Brazil, where significant IMs are evident. Figure 5a shows a line close to the Tupi discovery. A series of impedance contrasts can be observed such as the water bottom, top of salt (TOS), base of salt (BOS) and the layered salt structures. It will be difficult, if not impossible, to identify all the generators of the IMs, since many of them are closely packed. Moreover, the TOS is fairly rugose in both directions. Applying our method to attenuate the IMs and then performing migration on the resulted data, Figure 5b and 5c display the 2D and 3D IMA output, respectively. It can be observed that the migration swings, which are caused by the IMs, that interfere the interpretation of the BOS are much reduced in the 3D result.

CONCLUSIONS

We have described a 3D approach based on iteratively locating the multiple-generating horizons, while honouring the azimuths of the contributing traces, for predicting internal multiples. The method has been applied successfully in suppressing complex internal multiples that are generated by closely packed layered salt structures that exhibit significant 3D effects.

ACKNOWLEDGMENTS

The authors would like to thank CGGVeritas for permission to publish this work. Appreciation is also due to Stan Rob and Yan Huang for their help in generating the input datasets.

REFERENCES

El-Emam, A., and Al-Deen, K.S., Zarkhidze, A. and Walz, A., 2011, Advances in interbed multiples prediction and attenuation: Case study from onshore Kuwait: 81st Meeting, SEG Abstracts, 3546-3550.

Griffiths, M., Hembd, J. and Prigent, H., 2011, Applications of interbed multiple attenuation: *The Leading Edge*, 30, 906-912.

Hung, B. and Wang, M., 2012, Internal demultiple methodology without identifying the multiple generators: 82nd Meeting, SEG, Expanded Abstracts.

Jakubowicz, H., 1998, Wave equation prediction and removal of interbed multiple: 68th Meeting, SEG, Extended Abstracts, 1527-1530.

Lin, D., Young, J., Lin, W., Griffiths, M. and Hartmann, M., 2005, 3D SRME practice for better imaging: 67th Conference & Technical Exhibition, EAGE, Extended Abstracts, A030.

Moore, I., and Bisley, R., 2005, 3D surface-related multiple prediction (SMP): A case history: *The Leading Edge*, 24, 270-274.

Pica, A. and Delmas, L., 2008, Wave equation based internal multiple modeling in 3D: 78th Meeting, SEG, Expanded Abstracts, 2476-2480.

Reshef, M., Arad, S. and Landa, E., 2006, 3D prediction of surface-related and interbed multiples: *Geophysics*, 71(1), V1-V6.

Retailleau, M.G., Benjamin, N., Pica, A., Bendjaballah, M., Plasterie, P., Leroy, S., Delmas, L., Smith, R. and Shorter, J., 2011, Advanced 3D Land Internal Multiple Modeling and Subtraction, a WAZ Oman case study: 73rd Conference & Technical Exhibition, EAGE, Extended Abstracts.

Verschuur, D.J. and Berkhout, A.J., 2005, Removal of internal multiples with the common-focus-point (CFP) approach: Part 2 – Application strategies and data examples: *Geophysics*, 70, V61-V72.

Weglein, A. B., Gasparotto, F. A., Carvalho, P. M. and Stolt, R. H., 1997, An inverse-scattering series method for attenuating multiples in seismic reflection data: *Geophysics*, 62, 1975-1989.

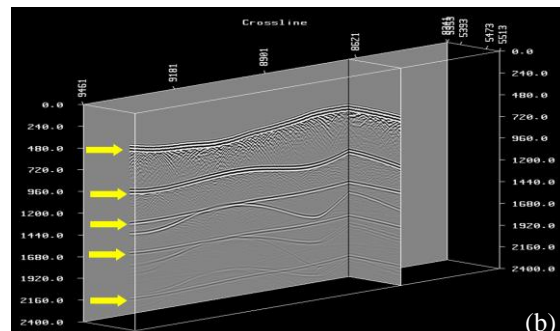
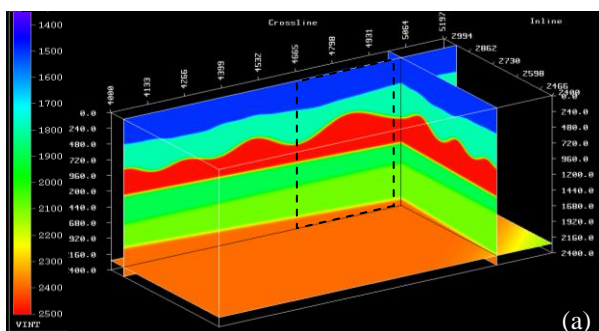


Figure 3. (a) 3D velocity profile for generating the synthetic data.(b) A portion of 3D offset cube with the five primary events highlighted by the arrows.

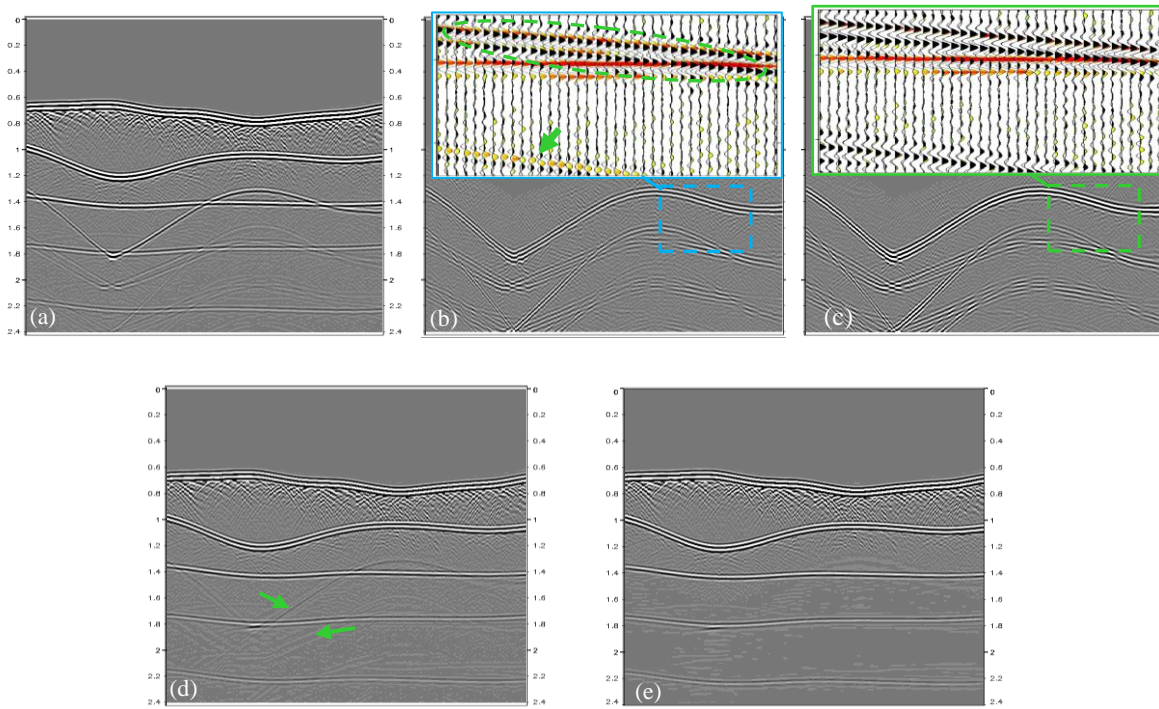


Figure 4. (a) Input near offset section before IMA. (b) 2D IM model. (c) 3D IM model. The wiggle displays show the overlay between the model and the input. (d) Subtraction result using the 2D model. (e) Subtraction using the 3D model.

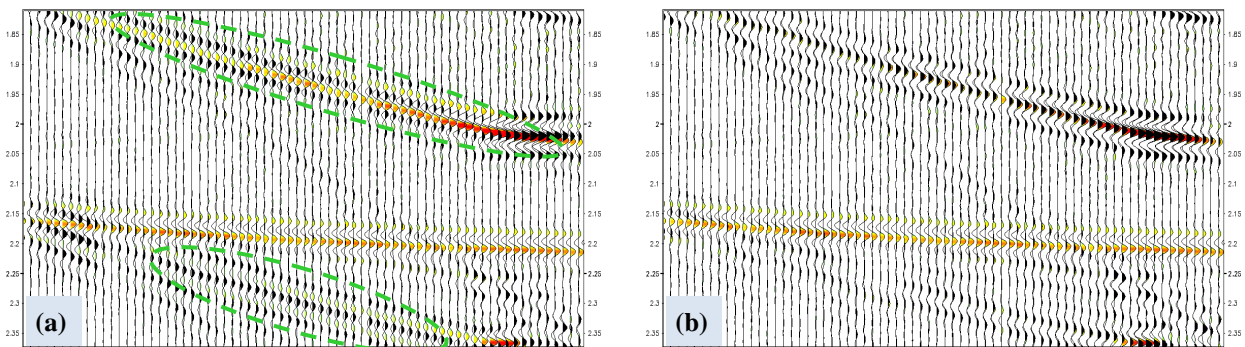


Figure 5. Overlay of the input (coloured wiggles) with the internal multiple model obtained by (a) prediction using nominal azimuths; and (b) prediction using true azimuths.

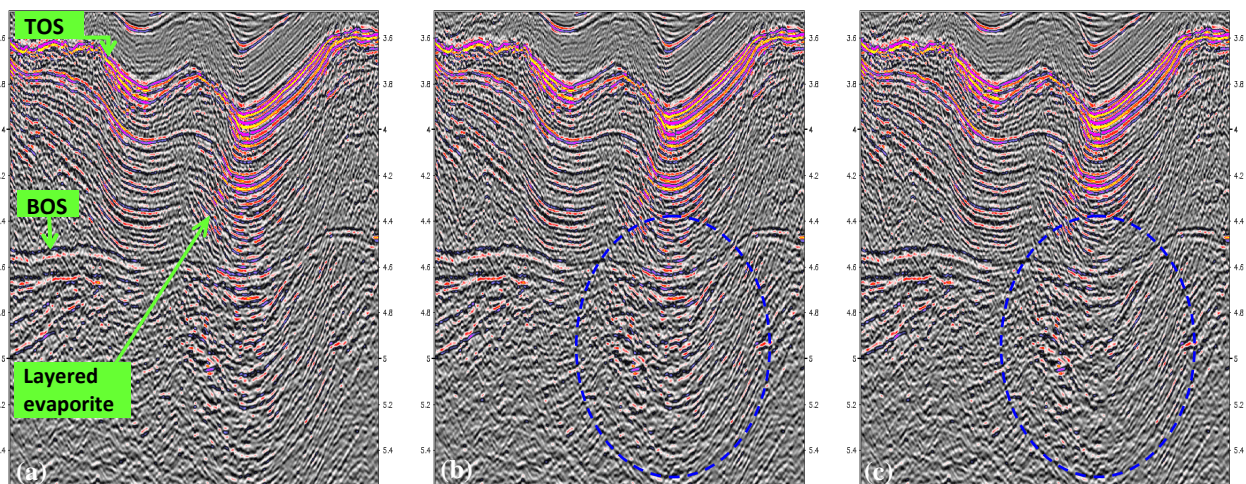


Figure 6. Migrated sections of a target line from the Santos Basin. (a) Input. (b) After 2D IMA. (c) After 3D IMA.